Supplementary Material: Improved Expressivity Through Dendritic Neural Networks

Xundong Wu **Xiangwen Liu** **Wei Li** **Qing Wu**
School of Computer Science and Technology
Hangzhou Dianzi University
Hangzhou, China
wuxundong@gmail.com, wuq@hdu.edu.cn

A Schematic drawing of neurons and their dendritic arbors

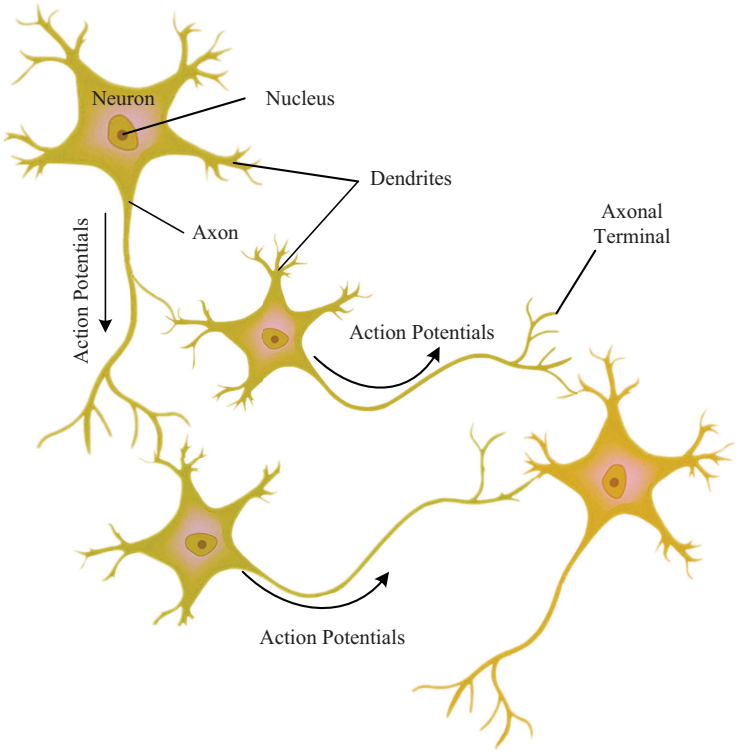

Figure A1: A schematic drawing of signal transmissions between neurons. It is shown that neurons receive synaptic inputs from proximity neurons on their dendritic arbors. Neurons then process synaptic inputs and send out action potential signals through their axons.

B Empirical Measurement of Network Complexity

For a fixed neural network of a certain architecture A, inputs x and parameters W, our aim is to know how the complexity of the network changes as A changes and across inputs x. But it is intractable to go over the entire input space. We study the complexity on a one dimensional *trajectories* through input space as in [2].

Definition 1 *For two points $x_0, x_1 \in \mathbb{R}^m$, a curve $x(t)$ parameterized by $t \in [0, 1]$, with $x(0) = x_0$ and $x(1) = x_1$ is called a trajectory between x_0 and x_1.*

If the activation function of a neural network is a piecewise linear function, the function it represents is also a piecewise linear function. And the number of linear pieces (regions) measures the complexity of a model.

Definition 2 *For a certain W, as inputs move from x to $x + \delta$, the piecewise linear activation function of a neuron switches into a different linear region. Then we define this is a neuron transition between x and $x + \delta$.*

A transition of a neuron with ReLU activation function would be given by a neuron switching from on to off (or vice versa) and for Maxout and DENNs by switching index of the maximum input branch. In this way we get the number of transitions undergone by output neurons as we sweep across any given input trajectory $x(t)$.

As in [2], we measure the complexity of the network by the number of neuron transitions. We empirically measure the number of transitions as we sweep x along $x(t)$ to learn its behavior and $x(t) = \cos(\pi t/2)x_0 + \sin(\pi t/2)x_1$, where x_0, x_1 are two different data points selected randomly from the MNIST dataset. The ReLU FNNs, DENNs, Maxout networks used in this study have two layers (The output layers for those networks are omitted since they don't use piece-wise activation functions.). For DENNs the branch number are set to $2^1, 2^2, \cdots, 2^8$ denoted by d. For the Maxout network, by increasing the number of kernels in a Maxout unit, the number of units is reduced accordingly to keep the total number of synaptic parameters constant. The network weights are randomly initialized with $\sim \mathcal{N}(0, 0.01)$.

As shown in Fig. A2, the transition counts of Maxout networks and DENNs grow as we shift toward larger branch numbers d. The transition counts of DENNs with any branch numbers are larger than that of Maxout networks and ReLU FNNs.

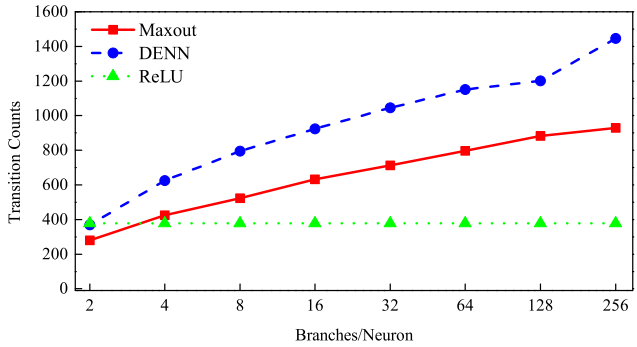

Figure A2: The transition counts of Maxout networks and DENNs with different branch numbers and the baseline ReLU FNN.

C Additional Results on Permutation Invariant Image Datasets

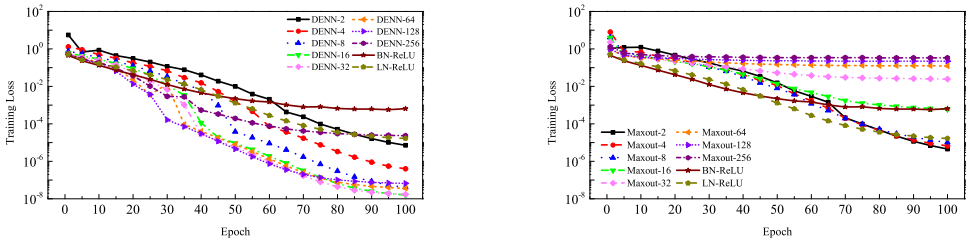

(a) (b)

Figure A3: Learning curves on Fashion-MNIST dataset. (a) Training loss curves on DENNs with different d and standard ReLU FNNs (BN-ReLU: batch normalization-ReLU; LN-ReLU: layer normalization-ReLU.). (b) Training loss curves on Maxout networks with different d and standard FNNs.

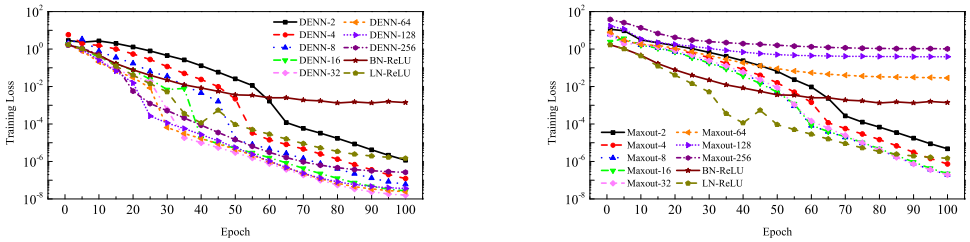

(a) (b)

Figure A4: Learning curves on CIFAR-10 dataset. (a) Training loss curves on DENNs of different d and standard FNNS. (b) Training loss curves on Maxout networks of different d and standard FNNs.

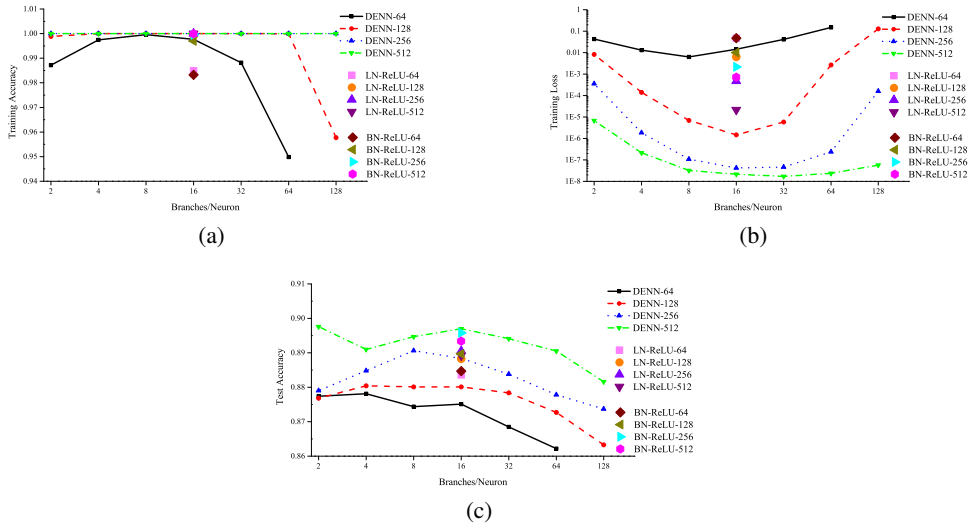

(a) (b)

(c)

Figure A5: Effect of varying the branch number and architecture on model behavior on Fashion-MNIST dataset (BN-ReLU: batch normalization-ReLU; LN-ReLU: layer normalization-ReLU.). (a) Training accuracy results. (b) Training loss results. (c) Test accuracy results.

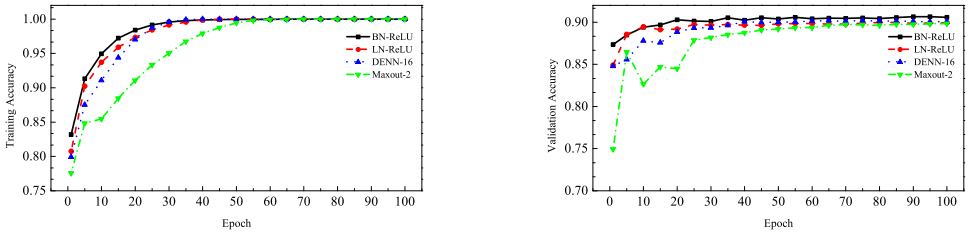

(a) (b)

Figure A6: Accuracy curves on Fashion-MNIST dataset for the DENN with $d = 16$, and the Maxout network with $d = 2$, along with ReLU FNNs (BN-ReLU: batch normalization-ReLU; LN-ReLU: layer normalization-ReLU.). (a) Training accuracy curves. (b) Validation accuracy curves

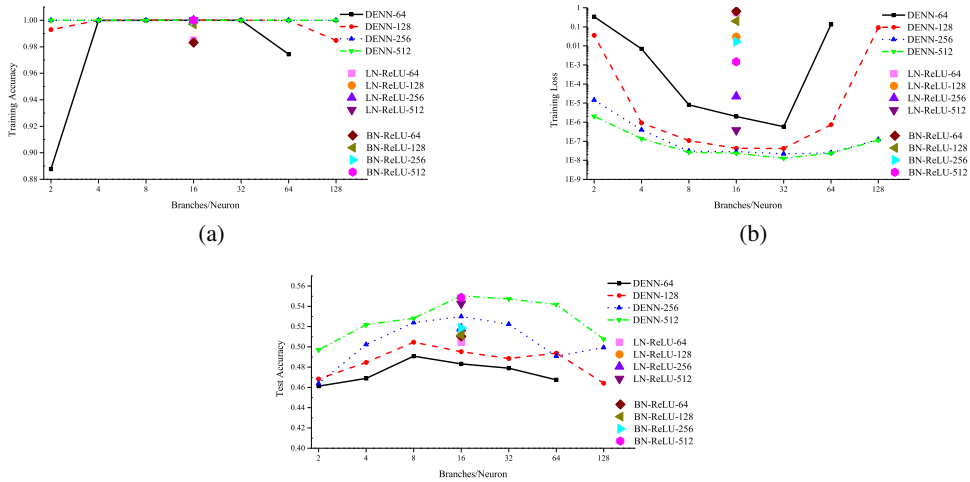

(a) (b) (c)

Figure A7: Effect of varying the branch number and architecture on model behavior on CIFAR-10 dataset (BN-ReLU: batch normalization-ReLU; LN-ReLU: layer normalization-ReLU.). (a) Best Training accuracy results. (b) Best training loss results. (c) Test accuracy results.

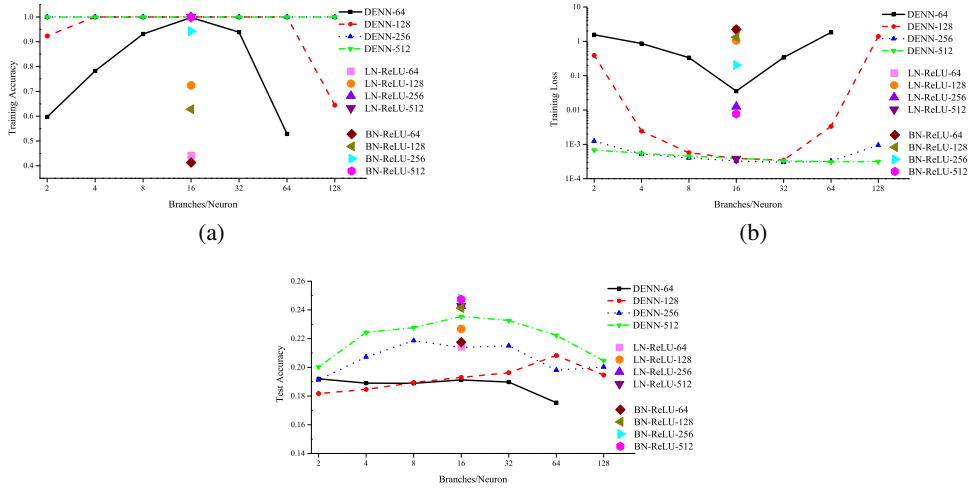

(a) (b) (c)

Figure A8: Effect of varying the branch number and architecture on model behavior on CIFAR-100 dataset (BN-ReLU: batch normalization-ReLU; LN-ReLU: layer normalization-ReLU.). (a) Best training accuracy results. (b) Best training loss results. (c) Test accuracy results.

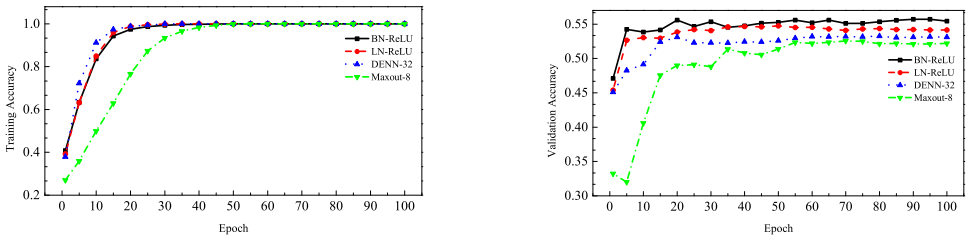

(a) (b)

Figure A9: Accuracy curves on CIFAR-10 dataset for the DENN with $d = 16$ and the Maxout network with $d = 2$ along with ReLU FNNs (BN-ReLU: batch normalization-ReLU; LN-ReLU: layer normalization-ReLU.). (a) Training accuracy curves. (b) Validation accuracy curves

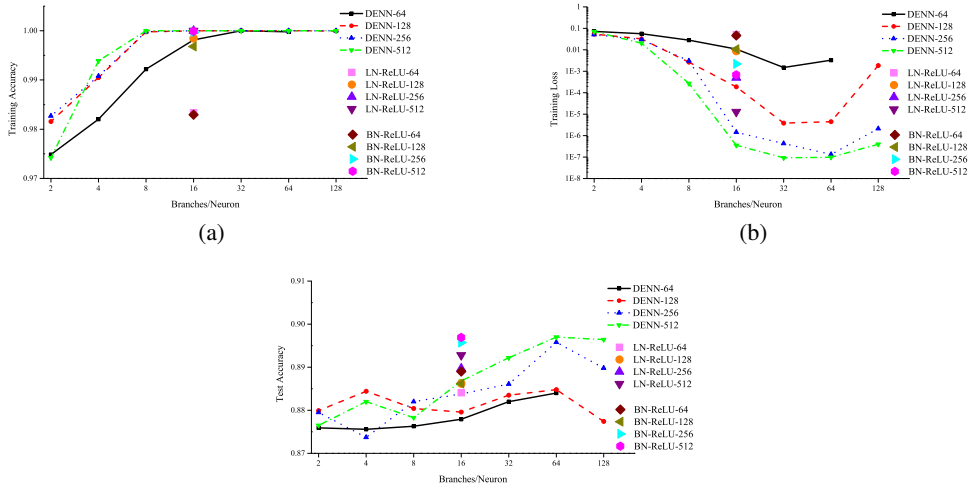

(a) (b)

(c)

Figure A10: Effect of varying the branch number and architecture on model behavior on FASHION-MNIST dataset (BN-ReLU: batch normalization-ReLU; LN-ReLU: layer normalization-ReLU.). DENNs here use a ReLU followed by an average-pooling instead of the Maxout for dendritic nonlinearity. (a) Training accuracy results. (b)Training loss results. (c) Test accuracy results.

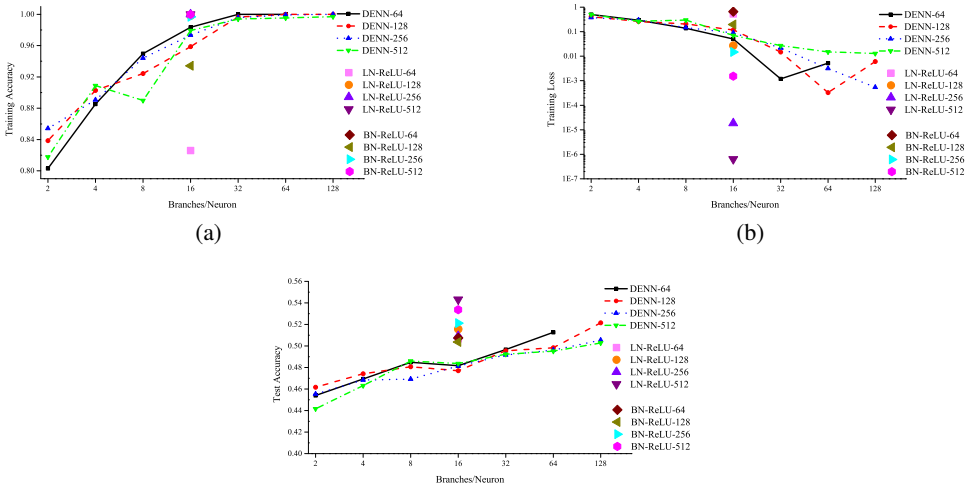

Figure A11: Effect of varying the branch number and architecture on model behavior on CIFAR-10 dataset (BN-ReLU: batch normalization-ReLU; LN-ReLU: layer normalization-ReLU.). DENNs here use a ReLU followed by an average-pooling instead of the Maxout for dendritic nonlinearity. (a) Training accuracy results. (b)Training loss results. (c) Test accuracy results.

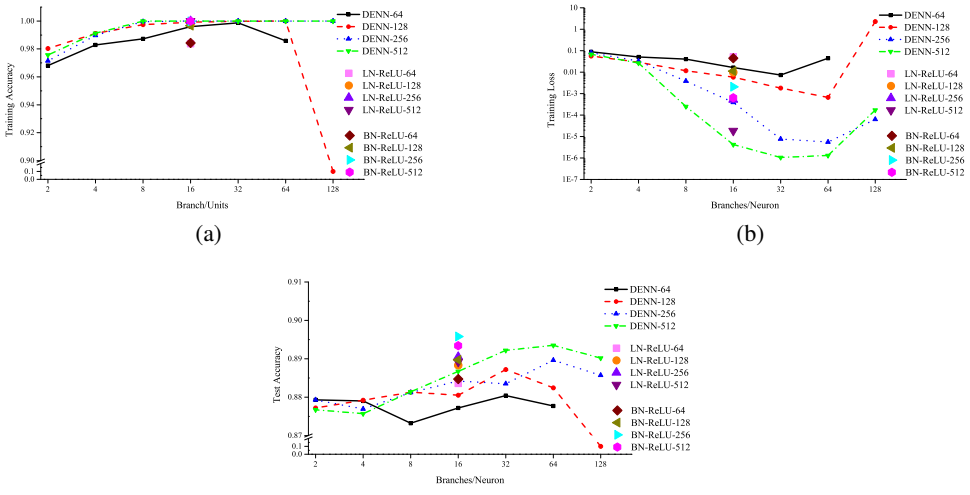

Figure A12: Effect of varying the branch number and architecture on model behavior on FASHION-MNIST dataset (BN-ReLU: batch normalization-ReLU; LN-ReLU: layer normalization-ReLU.). DENNs here use two ReLU nonlinearties instead of the Maxout for dendritic nonlinearity. (a) Training accuracy results. (b)Training loss results. (c) Test accuracy results.

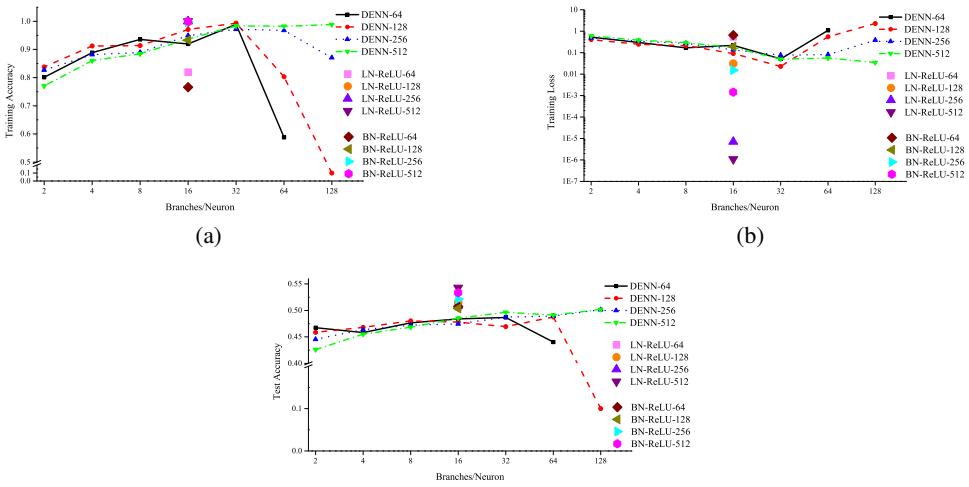

(a) (b) (c)

Figure A13: Effect of varying the branch number and architecture on model behavior on CIFAR-10 dataset (BN-ReLU: batch normalization-ReLU; LN-ReLU: layer normalization-ReLU.). DENNs here use two ReLU nonlinearties instead of the Maxout for dendritic nonlinearity. (a) Training accuracy results. (b)Training loss results. (c) Test accuracy results.

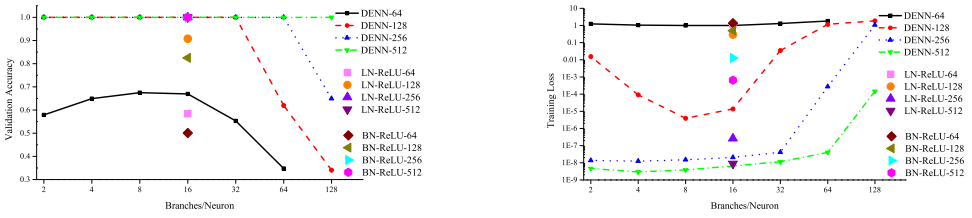

(a) (b)

Figure A14: Effect of varying the branch number and architecture on model behavior on random Gaussian noise data. (a) Training accuracy results. (b) Training loss results.

D Additional Results on 121 UCI Classfication Datasets

Table A1: Test accuracy of DENNs and SNNs, on every prediction task of 121 UCI datasets. The first column lists the name of the datasets, the second column and the third column are the number of samples N and the number of features M, the other columns are the test accuracy of DENNs, SNNs result from [1], and results from our implementation of SNNs. No significant difference is found between the result from our implementation of SNNs and that of the original authors.

Dataset	N	M	DENN	SNN	SNN-our
abalone	4177	8	0.6638	0.6657	0.6676
acute-inflammation	120	6	1	1	1
acute-nephritis	120	6	1	1	1
adult	48842	14	0.848	0.8476	0.8508
annealing	898	31	0.75	0.76	0.35
arrhythmia	452	262	0.6726	0.6549	0.6106
audiology-std	196	59	0.76	0.8	0.8
balance-scale	625	4	0.9808	0.9231	0.9679
balloons	16	4	1	1	1
bank	4521	16	0.8965	0.8903	0.8912
blood	748	4	0.7326	0.7701	0.738
breast-cancer	286	9	0.6901	0.7183	0.662
breast-cancer-wisc	699	9	0.9771	0.9714	0.9829
breast-cancer-wisc-diag	569	30	0.9859	0.9789	0.9648
breast-cancer-wisc-prog	198	33	0.7143	0.6735	0.7347
breast-tissue	106	9	0.6538	0.7308	0.6923
car	1728	6	0.9884	0.9838	0.9907
cardiotocography-10clases	2126	21	0.823	0.8399	0.8305
cardiotocography-3clases	2126	21	0.9435	0.9153	0.9322
chess-krvk	28056	6	0.8041	0.8805	0.8794
chess-krvkp	3196	36	0.9962	0.9912	0.9962
congressional-voting	435	16	0.578	0.6147	0.6055
conn-bench-sonar-mines-rocks	208	60	0.8269	0.7885	0.75
conn-bench-vowel-deterding	990	11	0.9935	0.9957	0.9935
connect-4	67557	42	0.8646	0.8807	0.8799
contrac	1473	9	0.5489	0.519	0.5598
credit-approval	690	15	0.8256	0.843	0.8314
cylinder-bands	512	35	0.7812	0.7266	0.75
dermatology	366	34	0.978	0.9231	0.956
echocardiogram	131	10	0.8788	0.8182	0.8485
ecoli	336	7	0.8571	0.8929	0.8452
energy-y1	768	8	0.9583	0.9583	0.9583
energy-y2	768	8	0.9062	0.9063	0.9219
fertility	100	9	0.88	0.92	0.88
flags	194	28	0.5208	0.4583	0.4375
glass	214	9	0.6038	0.7358	0.6038
haberman-survival	306	3	0.6579	0.7368	0.75
hayes-roth	160	3	0.8571	0.6786	0.7857
heart-cleveland	303	13	0.5789	0.6184	0.6053
heart-hungarian	294	12	0.7808	0.7945	0.7808
heart-switzerland	123	12	0.4839	0.3548	0.5161
heart-va	200	12	0.32	0.36	0.32
hepatitis	155	19	0.7949	0.7692	0.7179
hill-valley	1212	100	0.5462	0.5248	0.5066
horse-colic	368	25	0.8235	0.8088	0.8088
ilpd-indian-liver	583	9	0.7192	0.6986	0.7055
image-segmentation	2310	18	0.9057	0.9114	0.8967
ionosphere	351	33	0.9659	0.8864	0.8864
iris	150	4	1	0.973	0.973
led-display	1000	7	0.76	0.764	0.776

lenses	24	4	0.6667	0.6667	0.6667
letter	20000	16	0.962	0.9726	0.9766
libras	360	90	0.7778	0.7889	0.7778
low-res-spect	531	100	0.9023	0.8571	0.8872
lung-cancer	32	56	0.625	0.625	0.25
lymphography	148	18	0.9459	0.9189	0.9459
magic	19020	10	0.8681	0.8692	0.865
mammographic	961	5	0.8083	0.825	0.825
miniboone	130064	50	0.933	0.9307	0.9293
molec-biol-promoter	106	57	0.8846	0.8462	0.7308
molec-biol-splice	3190	60	0.8545	0.9009	0.857
monks-1	556	6	0.8171	0.7523	0.8819
monks-2	601	6	0.6505	0.5926	0.4861
monks-3	554	6	0.8009	0.6042	0.706
mushroom	8124	21	1	1	1
musk-1	476	166	0.8992	0.8739	0.8908
musk-2	6598	166	0.9927	0.9891	0.9915
nursery	12960	8	1	0.9978	0.9981
oocytes_merluccius_nucleus_4d	1022	41	0.8392	0.8235	0.8471
oocytes_merluccius_states_2f	1022	25	0.9294	0.9529	0.8863
oocytes_trisopterus_nucleus_2f	912	25	0.8246	0.7982	0.7851
oocytes_trisopterus_states_5b	912	32	0.9474	0.9342	0.9342
optical	5620	62	0.9638	0.9711	0.9716
ozone	2536	72	0.9748	0.97	0.9716
page-blocks	5473	10	0.9613	0.9583	0.9627
parkinsons	195	22	0.8571	0.898	0.8571
pendigits	10992	16	0.9737	0.9706	0.9714
pima	768	8	0.6979	0.7552	0.7552
pittsburg-bridges-MATERIAL	106	7	0.9231	0.8846	0.8462
pittsburg-bridges-REL-L	103	7	0.7308	0.6923	0.6923
pittsburg-bridges-SPAN	92	7	0.7391	0.6957	0.6957
pittsburg-bridges-T-OR-D	102	7	0.84	0.84	0.84
pittsburg-bridges-TYPE	105	7	0.5769	0.6538	0.6154
planning	182	12	0.6	0.6889	0.6889
plant-margin	1600	64	0.8325	0.8125	0.81
plant-shape	1600	64	0.725	0.7275	0.75
plant-texture	1599	64	0.81	0.8125	0.815
post-operative	90	8	0.6818	0.7273	0.6818
primary-tumor	330	17	0.5366	0.5244	0.5244
ringnorm	7400	20	0.9757	0.9751	0.9795
seeds	210	7	0.9231	0.8846	0.9423
semeion	1593	256	0.9673	0.9196	0.9296
soybean	683	35	0.8803	0.8511	0.8936
spambase	4601	57	0.9487	0.9409	0.9348
spect	265	22	0.6237	0.6398	0.6398
spectf	267	44	0.893	0.4973	0.5401
statlog-australian-credit	690	14	0.6105	0.5988	0.6395
statlog-german-credit	1000	24	0.72	0.756	0.744
statlog-heart	270	13	0.9254	0.9254	0.8955
statlog-image	2310	18	0.9775	0.9549	0.9532
statlog-landsat	6435	36	0.899	0.91	0.912
statlog-shuttle	58000	9	0.9991	0.999	0.9989
statlog-vehicle	846	18	0.8104	0.8009	0.8009
steel-plates	1941	27	0.7753	0.7835	0.7732
synthetic-control	600	60	0.9933	0.9867	0.9933
teaching	151	5	0.5789	0.5	0.6053
thyroid	7200	21	0.9822	0.9816	0.977
tic-tac-toe	958	9	0.9833	0.9665	0.9833
titanic	2201	3	0.7873	0.7836	0.7836

trains	10	29	NA	NA	NA
twonorm	7400	20	0.9816	0.9805	0.9795
vertebral-column-2clases	310	6	0.8571	0.8312	0.8442
vertebral-column-3clases	310	6	0.8052	0.8312	0.8442
wall-following	5456	24	0.9186	0.9098	0.9091
waveform	5000	21	0.8392	0.848	0.8792
waveform-noise	5000	40	0.8432	0.8608	0.852
wine	178	13	1	0.9773	0.9545
wine-quality-red	1599	11	0.635	0.63	0.645
wine-quality-white	4898	11	0.6225	0.6373	0.6242
yeast	1484	8	0.5822	0.6307	0.6065
zoo	101	16	1	0.92	0.96

References

[1] Günter Klambauer, Thomas Unterthiner, Andreas Mayr, and Sepp Hochreiter. Self-normalizing neural networks. In *Advances in Neural Information Processing Systems*, pages 972–981, 2017.

[2] Maithra Raghu, Ben Poole, Jon Kleinberg, Surya Ganguli, and Jascha Sohl-Dickstein. On the expressive power of deep neural networks. In *International Conference on Machine Learning*, pages 2847–2854, 2017.